[redacted]

HW-34509
REACTORS - PRODUCTION
SPECIAL DISTRIBUTION

COPY NO. 11 [redacted]

PHYSICS RESEARCH QUARTERLY REPORT

OCTOBER, NOVEMBER, DECEMBER

1954

BY

THE STAFF OF PHYSICS RESEARCH

PILE TECHNOLOGY SECTION
ENGINEERING DEPARTMENT

JANUARY 20, 1955

[redacted]

THIS DOCUM[redacted] CONTAIN[redacted]ESTRICTE[redacted]AS
[redacted]ED IN T[redacted]IC EN[redacted]CT OF [redacted] ITS CO[redacted]
TENTS IN[redacted]ANNE[redacted]Y U[redacted]ORIZED
PERSON IS PROH[redacted]TED.

HANFORD ATOMIC PRODUCTS OPERATION
RICHLAND, WASHINGTON

GENERAL ELECTRIC

A.E.C. - G.E. - RICHLAND, WASH.

[redacted]

HW-34509

GENERAL ELECTRIC COMPANY

AEC RESEARCH AND DEVELOPMENT REPORT

RICHLAND, WASHINGTON — HANFORD ATOMIC PRODUCTS OPERATION

QUARTERLY REPORT

HW--34509

DE87 006760

PHYSICS RESEARCH SUB-SECTION

October, November, December, 1954

by

The Staff of the Physics Research Sub-Section

Pile Technology Section
ENGINEERING DEPARTMENT

January 20, 1955

HANFORD ATOMIC PRODUCTS OPERATION
RICHLAND, WASHINGTON

Operated for the Atomic Energy Commission by the
General Electric Company under Contract W-31-109-Eng-52

G-1532. 1-D

[redacted]

GENERAL ELECTRIC
COMPANY

[redacted]

-1-

DECLASSIFIED

HW-34509

Reactors - Production
Special Distribution

RICHLAND, WASHINGTON . . . . HANFORD ATOMIC PRODUCTS OPERATION

This document consists of 46 pages. ~~Copy No. 11 of 124~~ copies. Series [redacted]

QUARTERLY REPORT

PHYSICS RESEARCH SUB-SECTION

October, November, December, 1954

by

The Staff of the Physics Research Sub-Section

Pile Technology Section
ENGINEERING DEPARTMENT

CLASSIFICATION CANCELLED
Per DOE 1973
By L. Pope 12/18/74
JE Savely 6-5-02

January 20, 1955

HANFORD ATOMIC PRODUCTS OPERATION
RICHLAND, WASHINGTON

Operated for the Atomic Energy Commission by the
General Electric Company under Contract W-31-109-Eng-52

[redacted]

[redacted]is document [redacted] Data as defined in [redacted] manner [redacted]hibited.

WARNING - PRELIMINARY REPORT

This report contains information of a preliminary nature and is prepared primarily for the use of Hanford Works Pile Technology Section Personnel. This report is subject to revision on further checking or collection of additional data.

DECLASSIFIED

[redacted]

INTERNAL DISTRIBUTION

Copy Number

1. FW Albaugh
2. RK Andersen
3. GW Anthony
4. PM Anselone - MC McGee
5. CA Bennett
6. RA Bennett
7. EZ Block
8. LP Bupp
9. SH Bush - MJ Sanderson
10. JJ Cadwell - OJ Wick
11. ED Clayton
12. JB Czirr
13. DE Davenport
14. MV Davis - HA Fowler
15. DJ Donahue - DD Lanning
16. WB Farrand
17. JE Faulkner
18. WJ Friesen
19. GC Fullmer
20. PF Gast
21. OH Greager
22. RE Heineman
23. HL Henry
24. EE Jones
25. HW Lefevre
26. BR Leonard
27. WR Lewis
28. RC Lloyd
29. WM Mathis - WW Windsheimer - EW O'Rorke
30. RE McGrath - AP Vinther
31. EB Montgomery
32. GM Muller
33. H Neumann
34. JD Orton - RR Bloomstrand
35. GF Owsley - GB Coover
36. WJ Ozeroff
37. RE Peterson
38. WH Reas - RJ Brouns - FJ Leitz - HH Hopkins
39. RL Dickeman
40. CR Richey
41. EJ Seppi
42. DF Snoeberger
43. WP Stinson
44. GW Stuart
45. JR Triplett
46. LD Turner
47. JH Warren - RO Mehann
48. 300 File
49. Yellow Copy

EXTERNAL DISTRIBUTION

Copy Number

50-60	Argonne National Laboratory
61	Argonne National Laboratory, Attn: J.M. West, R.J. Haydn
62	Armed Forces Special Weapons Project, Washington
63-67	Atomic Energy Commission, Washington
68	Battelle Memorial Institute
69	Brookhaven National Laboratory
70	Brookhaven National Laboratory, Attn: J. Chernick, J.A. Harvey
71	Bureau of Ships
72-77	Carbide and Carbon Chemicals Company (ORNL)
78	Chicago Patent Group
79-82	duPont Company, Augusta
83	duPont Company, Augusta, Attn: C.W.J. Wende
84	duPont Company, Wilmington
85	General Electric Company (ANPD), Attn: F. Metzger
86	Hanford Operations Office
87-88	Knolls Atomic Power Laboratory
89	Knolls Atomic Power Laboratory, Attn: L. Tonks, T.M. Snyder
90-91	Los Alamos Scientific Laboratory
92	Los Alamos Scientific Laboratory, Attn: R.F. Taschek, C.W. Zabel
93	Massachusetts Institute of Technology (Benedict)
94-95	North American Aviation, Inc.
96	North American Aviation, Attn: S. Siegel
97	Patent Branch, Washington
98-101	Phillips Petroleum Company (NRTS)
102	San Francisco Operations Office
103	USAF Headquarters
104-105	University of California Radiation Laboratory, Berkeley
106-107	University of California Radiation Laboratory, Livermore
108-109	Westinghouse Electric Corporation
110-124	Technical Information Service, Oak Ridge

TABLE OF CONTENTS

TABLE OF CONTENTS (cont'd)

SUMMARY

A revised calculation of the contribution of plutonium to the temperature coefficient of graphite piles is given. An experiment in the Lattice Testing Reactor to measure this contribution is described. An outline is given of a new and more accurate method of calculating temperature coefficients of reactivity and isotope buildup. The method of successive generations is extended to include the neutron flux in the moderator of a pile in order to permit the calculation of thermal utilization. The temperature of the neutron flux leaving a Hanford-type slug is calculated. Buckling measurements are reported on slugs possessing axial holes filled with water. A description of two inexpensive neutron sources is given. Measurements are reported on the resonance integral of U-235.

Techniques are described for the measurement of $\bar{\nu}$(U-235) at thermal energy and some preliminary results are given. Progress on the measurement of the C-12 and Th-232 cross sections and related work is reported.

An outline is given of a method for calculating the changes in the thermal properties of a crystal caused by the presence of randomly placed impurities.

Some estimates of "critically safe" cylinders are made for very concentrated plutonium solutions in which the flux is faster than thermal.

LATTICE PHYSICS

The Dependence of Long Term Reactivity Gains on Neutron Temperature and the Variation of the Graphite Temperature Coefficient with Exposure - R. E. Heineman

The calculations presented in the previous Quarterly Report, HW-33384, and at the recent Reactor Physics Conference at the Oak Ridge National Laboratory have been revised in part and such portions are presented here. Though the magnitude of the temperature effects on reactivity are changed somewhat, their trend is the same. These revised numbers are presented specifically to give some idea of the order of magnitude of the effects, their uncertainties, and their trend. More exact calculations are necessary, which make use of values of α_{49} in the 0.3 ev resonance that are more certain than the values calculated in BNL-250, in order to predict initial reactivity gains with assurance.

In the previous calculations the cross sections used were average values over the pile spectrum (thermal + 1/E tail) for a reactor having unirradiated fuel. These cross sections were not changed as a function of exposure. Since the pile cross section of U-238 is, for example,

$$\sigma^{28}_{pile} = \sigma^{28}_{thermal} + \xi(1 - p_{28})\left(\nu^{25}\sigma_f{}^{25}\frac{N^{25}}{N^{28}} + \nu^{49}\sigma_f{}^{49}\frac{N^{49}}{N^{28}}\right)$$

which increases with exposure of the fuel, neglecting this variation gives a reactivity gain with exposure which is too large. Neglecting the similar changes in the 49 cross sections gives a gain which is too small. The overall effect is that too large a reactivity gain was predicted. In the revised calculations the correct pile cross section of 28 is used in calculating the buildup of Pu-239, but only the thermal part is used in the determination of the change in multiplication factor. The resultant equation for the initial slope of the local long term gains curve is

$$A(T,T') = 6.02(1 + \alpha_{25})\left\{Co(T)\frac{\sigma_f{}^{49}(T')}{\sigma_f{}^{25}(T')}\left[\frac{\nu^{49}}{\nu^{25}} - \frac{1 + \alpha_{49}(T')}{1 + \alpha_{25}}\right] - \frac{Co_{th}(T') + \dfrac{\sigma_a{}^{p}(T')/\sigma_a{}^{25}(T')}{1 + \alpha_{25}}}{1 + Co_{th}(T')}\right\}$$

where $A(T,T')$ is the slope in ih/MWD/T for a reactor which is operated at temperature T and whose reactivity is measured at temperature T'; Co is the initial conversion ratio; Co_{th} is the thermal part of the conversion ratio; and $\sigma_a{}^{p}$ is the fission product absorption cross section per fission pair (neglecting Xe-135 and Sm-149). This equation is the same as that given by J. B. Sampson[1] except that the contribution of changes in thermal utilization are not included here.

There are three factors which contribute to an uncertainty in predicting the initial slope for a Hanford-type reactor. They are: 1) the effective neutron temperature

(1) J. B. Sampson, NAA-SR-195, Reactor Physics Conference (1951), p. 49

is not known; 2) the pile average α_{49} is probably rather uncertain; and 3) the value of the average fission product cross section has never been determined within, perhaps, a factor of two.

The curves of A(T,T') plotted in Figure 1 therefore use neutron temperature as a parameter and are plotted for various assumptions concerning the values of α_{49} and σ_a^p. The pile average values of α_{49} which are used are plotted in Figure 2. The curves labeled BNL-250 are determined from the f factors for 49 absorption and fission and from measured piles values of $\sigma_f^{49}/\sigma_f^{25}$ as a function of temperature. The humped character of the curve is attributed to the fact that the 49 absorption and fission cross sections have been measured with different resolution. The second curve for α_{49} has been smoothed and lowered by an arbitrary amount to show the effect of a change in α_{49} in the 0.3 ev resonance.

The initial slope of the local long term gains taken at the startup of the Hanford H-Pile is reported[1] to be 1.25 ih/MWD/T. Since the graphite temperature coefficient of reactivity was not determined as a function of exposure, this value should correspond to that for the hot pile. Thus, a search through the records should be made to determine the moderator temperatures during the time the H-Pile data was being taken. This, together with data on the production of Pu-240 at the pile areas, should shed some light on the question of α_{49} and the effective neutron temperature.

An analysis of the percent Pu-240 found in Hanford plutonium yields, essentially, the cross-section ratio $\frac{\overline{\sigma_c^{49}}}{\overline{\sigma_f^{25}}} = \frac{\overline{\sigma_f^{49}}}{\overline{\sigma_f^{25}}}\,\overline{\alpha_{49}} = 0.984$. Using a reasonable value for neutron temperature, 600°K (about 50°K less than the maximum graphite temperature) in assigning a value to the ratio $\frac{\overline{\sigma_f^{49}}}{\overline{\sigma_f^{25}}}$, one finds a value of $\overline{\alpha_{49}}$ of 0.46. Lowering the temperature by 100° to 500°K gives $\overline{\alpha_{49}} = 0.52$. Thus, lowering the assumed effective temperature increases the derived value of $\overline{\alpha_{49}}$. On the other hand, from Figure 1 it is seen that increasing the assumed neutron temperature for a given initial slope A(T=T') increases the value of $\overline{\alpha_{49}}$.

The calculated initial slopes imply an increasing graphite temperature coefficient of reactivity, Cg, with exposure. The change is given by

$$\Delta\, Cg = \frac{A(T = T') - A(T,300)}{T - 300} \text{ ih/°C/MWD/T.}$$

For T = 500° Figure 1 gives values of Δ Cg of 2.2×10^{-3} or 3.0×10^{-3} ih/°C/MWD/T for the two sets of values of $\overline{\alpha_{49}}$. Δ Cg increases as the temperature T increases. The implications of a large temperature coefficient on reactor control due to the Pu-239 contained in either a high temperature, high exposure power reactor using U-238 in its fuel or a high temperature Pu-239 enriched reactor has been pointed out in an internal memorandum.[2] The calculations which have been presented here

(2) HW-33789, Factors Limiting High Exposure Operation of the Proposed Dual Purpose Reactor, R. E. Heineman and G. W. Stuart.

Figure

EXAMPLE σ_{49} VALUES

PILE AVERAGE σ_{49} - BNL 250

σ_a^P = 56 barns

σ_a^P = 40

H-pile

A (ih/MWD/T)

3.0

2.0

1.0

0

300 400 500 600 700 800

T (°K)

——— A(T=T')

- - - - A(T, 300)

Figure 2

are not the most suitable for temperature coefficient calculations, as has been pointed out by G. W. Stuart, and an exact calculation for high exposure fuel should take into account the self-shielding in the vicinity of the Pu-239 resonance.

Though the change in Cg due to Pu-239 buildup in a Hanford reactor is rather sizable even at 600 MWD/T, it has never been observed conclusively. In the first place such a change has never been looked for and, in the second place, the temperature coefficient should be expected to decrease initially while the Sm-149 builds up to saturation. Under such conditions, and realizing the difficulty of observing temperature coefficient changes under operating conditions, it is not surprising that such expected changes have not been observed in the routine operation of the Hanford reactors.

Prototype Lattice Testing Reactor - D. J. Donahue, D. D. Lanning

Consideration has been given to the possibility of measuring in the LTR the variation of the moderator temperature coefficient of reactivity of graphite piles with the exposure of the fuel in the pile. Calculations(3) have shown that this variation may be quite large and significant in the design of high exposure piles.

Preliminary steps have been taken toward the procurement of uranium slugs alloyed with varying amounts of plutonium. The Pu-239 and U-235 concentrations in these slugs will be adjusted to simulate natural uranium which has an integrated exposure of 0, 1000, 2000, and 4000 MWD/T. No effort will be made, during the fabrication of these slugs, to actually duplicate the distribution of Pu in an irradiated slug, but rather, the Pu will simply be dispersed homogeneously throughout.

Core Heater for LTR - R. E. Peterson

In order that temperature effects in a test lattice may be measured in the proposed experiments for the prototype LTR, methods for elevating the temperature of the test core are being considered. Meaningful measurements can be made only if the core is thermally insulated from the remainder of the reactor. An upper temperature limit of 400 C has been tentatively decided upon for the core. The design may then be resolved into the following broad specifications:

i) Provide means for introducing heat energy into the test core uniformly, utilizing a low neutron absorbing medium with the core in place in the reactor.

ii) Provide a thermal barrier between the test core and the remainder of the reactor such that the latter remains at essentially ambient temperature, also utilizing a low neutron absorbing medium.

iii) Provide instrumentation to control and measure core temperature accurately.

---

(3) HW-32934, The Dependence of Long Term Gains on Neutron Temperature, and the Variation of the Graphite Temperature Coefficient with Exposure, R. E. Heineman

Heat energy may be introduced into the core by either circulating a heat transferring medium or by electrical resistance heating. At the present time resistance heating appears to be most convenient. Resistance heating elements of the "Cal Rod" type are being considered.

The thermal barrier presents a more difficult problem from an engineering viewpoint. It appears that a vacuum envelope on all six sides of the core, made of aluminum whose walls are supported by small ceramic pieces, will meet the specification set forth.

Rough calculations indicate that the energy required to raise the core temperature to 400 C is of the order of 200 KWH. Plans have been made to mock-up the designs on a laboratory scale and measure the heat leakage, temperature distribution, etc., prior to building the full scale unit.

β Weighting, Temperature Coefficients of Reactivity and Isotope Buildup Calculations - G. W. Stuart

I. In this report we shall discuss certain aspects of the three rather unrelated topics appearing in the title. This seeming diversity of content is removed and all are concatenated into a cohesive whole upon the introduction of the somewhat protean problem which initially stimulated our investigation.

When there is a high inventory of Pu-239 in a thermal reactor operating on a uranium-plutonium cycle, the reactor will possess a massive positive temperature coefficient of the regeneration factor η, making reactor control a fairly difficult task. The reader may substantiate the foundation of our argument by consulting the Pu-239 cross sections in BNL-250. The rather large low lying resonance in the Pu-239 cross section at 0.3 ev is the culprit in this instance. Our problem, mentioned in the paragraph above, is to accurately calculate the magnitude of this effect for the geometry (cylindrical fuel elements) and isotopic concentrations of interest to Hanford.

II. β Weighting

For our first consideration, let us examine the established method of averaging η over energy, i.e., over a maxwellian distribution of thermal neutrons. This involves multiplying the monoenergetic value $\eta(E)$ by the probability of capture at that energy $\Sigma^a(E)$ (the macroscopic absorption cross section) and the number of neutrons present at that energy, $\phi(E,kT)$, taken to be maxwellian. Integration over energy and division by the normalizing factor, yields

$$\langle \eta \rangle_{kt} = \frac{\int_0^\infty \eta(E)\Sigma^a(E)\phi(E,kT)\,dE}{\int_0^\infty \Sigma^a(E)\,\phi(E,kT)\,dE} \qquad (1)$$

$$\Sigma^a(E) = \sum_i \Sigma_i^a(E)$$

where the sum is over the various isotopes. Introducing the definition of η (E)

$$\eta(E) = \frac{\sum_i \nu_i \Sigma_i^f (E)}{\sum_i \Sigma_i^a (E)} \tag{2}$$

and that of "f" factors

$$f_i^{a,f} = \frac{\int_o^\infty \Sigma_i^{a,f} (E)\, \phi(E)\, dE}{\frac{\sqrt{\pi}}{2} \Sigma_i^{a,f} (kT)} \tag{3}$$

reduces Equation 1 to the well-known form

$$\langle \eta \rangle_{kT} = \frac{\sum_i \nu_i f_i^f (kT)\, \Sigma_i^f (kT)}{\sum_i f_i^a (kT)\, \Sigma_i^a (kT)} \tag{4}$$

Equation 4 is clearly not applicable to the problem at hand. Consider the pathological situation where our maxwellian distribution is centered at thermal energy with an infinite resonance (of finite width) appearing in an isotopic cross section at 10^{20} ev. From Equation 3 the relevant "f" factor would be infinite. This is ridiculous for we cannot absorb, at a given energy more neutrons than are present at that energy. Alternately stated, Equation 3 does not account for the flux depression within an absorbing medium. Let us reformulate the problem by substituting $\beta(E)$ for $\Sigma^a(E)$ where $\beta(E)$ is the blackness of the fuel rod[4] to neutrons of energy E, i.e., the probability that a neutron of energy E incident upon the fuel rod will be absorbed.

$$\langle \eta \rangle_{kT} = \frac{\int_o^\infty \eta(E)\, \beta\, (E)\, \phi\, (E,kT)\, dE}{\int_o^\infty \beta\, (E)\, \phi\, (E,kT)\, dE} \tag{5}$$

This formulation is by definition, providing $\beta(E)$ is calculated correctly, the proper one. Since $\beta(E)$ refers to impinging neutrons $\phi(E,kT)$ need only refer to the incident neutron spectrum which is to a high approximation maxwellian.[5] The so-called spectral hardening effect of the neutron

(4) Rod blacknesses are plotted as a function of rod cross section and dimension in HW-34187. The theory underlying these values may be found in HW-33566.

(5) See The Exit Thermal Neutron Spectrum from a Hanford Slug , elsewhere in this Quarterly Report.

spectrum within the fuel rod is incorporated into Equation 5. Furthermore, for a very highly absorbing rod $\beta(E)$ saturates to unity eliminating the anomalous situation where more neutrons are absorbed than are present.

One can now see that Equation 1 is applicable only in the case of small rod absorption, i.e.,

$$\beta(E) \xrightarrow[\Sigma^a(E) \to 0]{} \Sigma^a(E) \tag{6}$$

Substitution of β weighting for Σ^a weighting will reduce the influence of the Pu-239 resonance by reason of the saturability of β and thus decrease the temperature coefficient of η.

III. The Spatial Distribution of Isotopes

In our program to accurately tie down the temperature coefficient of η for a high exposure reactor we must take into account the spatial distribution of isotopes within a fuel rod. Since Pu-239 builds up roughly as $Io(\kappa r)$, being peaked towards the outside of the rod, whereas the residual U-235 distribution has exactly the opposite behavior, and since the thermal flux also rises towards the periphery of the rod, one would expect the Pu-239 contribution to η to be emphasized while the U-235 contribution is de-emphasized. The U-238 distribution may be taken as flat so that it also will be de-emphasized. Because the monoenergetic flux shape, $\phi(E,r)$, within the rod differs from energy to energy, one can see that the above effect will be temperature dependent. The isotope distribution effect will increase the influence of the Pu-239 resonance since within the energy range of the resonance the flux distribution within the rod will be quite steep.

It will now be necessary to put the above discussion into mathematical terms. Assume that the radial distribution of isotope i within a fuel rod is given by $\lambda_i(r)$. We define a function $q_i(E)$ by

$$q_i(E) = \frac{\text{absorptions in isotope i at energy E}}{\text{absorptions in isotope i at energy E with a flat spatial distribution}} \tag{7}$$

so that we may redefine η as

$$\eta(E) = \frac{\sum_i \nu_i \, q_i(E) \, \Sigma_i^f(E)}{\sum_i q_i(E) \, \Sigma_i^a(E)} \tag{8}$$

Equation 7 may be restated

$$q_i(E) = \frac{\int d\vec{r} \int \lambda_i(r) \, \phi(E,r) \, d\vec{r}}{\int \lambda_i(r) d\vec{r} \int \phi(E,r) d\vec{r}} \tag{9}$$

[redacted]

In practice, one will obtain the flux distributions, $\phi(E,r)$, from the successive generations method (HW-33566; loc. cit.). Since these distributions are calculated on the basis of a homogeneous rod, such a substitution corresponds to a first order perturbative approximation. This approximation will underestimate q for Pu-239 and overestimate q for U-235 thus underestimating the η effect. The $\lambda_i(r)$ have been experimentally determined at Hanford.

Equation 8 is used to replace Equation 2 in Equation 5.

IV. Isotope Buildup Calculations

The final topic we shall consider here is that of isotope buildup calculations. In order to obtain effective cross sections for this type calculation, we must both β-weight and q-weight. Again, casting our statements into mathematical form.

$$(10) \qquad \langle \sigma_i \rangle = \frac{\int_0^\infty q_i(E)\, \sigma_i(E)\, \phi(E,kT)\, \beta(E)\, dE}{\int_0^\infty \phi(E,kT)\, \beta(E)\, dE}$$

It should be noted that since β and q_i are functions of all the isotopes present in the rod $\langle \sigma_i \rangle$ will also be dependent upon the nuclear species different from i. In addition, β (and q_i) will be functions of exposure so that, a fortiori, $\langle \sigma_i \rangle$ will vary with irradiation.

To make the calculation tractable, β will be taken from the homogeneous rod calculation.

Thermal Utilization and Slug Blackness - G. W. Stuart

A rigorous transport theoretic method, the method of successive generations, has been formulated[6] which yields a complete description of the thermal neutron behavior within a cylindrical fuel rod. It is now necessary to continue this solution out into the graphite in order to calculate thermal utilizations. The pedestrian route to this end is to:

i) Use the ordinary diffusion theory functional form[7] in the moderator:

$$(1) \qquad \phi_1(r) = C\left[I_o(\kappa_1 r)K_1(\kappa_1 R_1) + K_o(\kappa_1 r)I_1(\kappa_1 R_1)\right] + S, \text{ and}$$

ii) Employ the rigorous fuel rod solution to modify the boundary conditions satisfied by the moderator solution at the fuel rod moderator interface.

---

(6) HW-29992, HW-31351, HW-32349, HW-33566. The most complete description is given in HW-33566, G. W. Stuart and R. W. Woodruff, The Successive Generations Method.

(7) Glasstone, Elements of Nuclear Reactor Theory, p. 268, eq. (9.59.1). Glasstone's notation will be used throughout except for some obvious changes.

This is the program we shall outline below.

Instead of applying a boundary condition on the net current crossing the interface, we instead apply a boundary condition on the inward current. (Continuity of net current is also contained in Equation 2 below by reason of the definition of rod blackness.)

$$J_{IN} = \frac{\phi_1}{4} + \frac{D_1}{2} \left.\frac{\partial \phi_1}{\partial r}\right|_{R_o} \tag{2}$$

This expression for the current is consistent with the assumption of a hemispherically symmetric entering current made in the successive generations calculation within the slug. We retain continuity of flux as our other boundary condition.

$$\phi_1(R_o) = \zeta J_{IN} \tag{3}$$

where[8]

$$\zeta = \sum_n (\Sigma_{so} R_o)^n \, II_n \, (1,x) \tag{4}$$

Upon using the definition

$$\frac{1}{f} = 1 + \frac{\text{absorptions in moderator}}{\text{absorptions in metal}} \tag{5}$$

and recognizing that absorptions in metal equals $2\pi R_o J_{IN} \beta$, where β is slug blackness, one obtains upon elementary integration and algebraic manipulation,

$$\frac{1}{f} = 1 + \frac{\Sigma_{a1} V_1}{\Sigma_{ao} V_o} F + G(E-1) \tag{6}$$

where

$$F = \frac{\zeta \, \Sigma_{ao} R_o}{2\beta} \tag{7}$$

$$G = \frac{2}{\beta} \left(1 - \frac{\zeta}{4}\right) \tag{8}$$

and E has the standard diffusion theory form.

The function G is new, not having appeared in the slightly less sophistacted forms of the theory. It may be interpreted as follows: Upon introducing ζ into the problem, we no longer had to stipulate the form of the exit neutron current. This was a favorable modification since the exit neutron current distribution, in distinction to the entering distribution, is far from assuming the diffusion theoretic

(8) This is Equation 16, p. 12, HW-33566 evaluated at T = 1.

form for a reasonably strong absorber. The function G accounts in part for the higher angular harmonics in the exit current distribution. To secure the rest of the effect, one would have to replace Equation 1 with a more accurate form, i.e., modify E. This could be done by employing a hemispherical harmonic solution in the moderator since the various angular moments of the exit neutron distribution fall out of the successive generations treatment.

By combining Equations 7 and 8 we may eliminate ζ and cast G into a slightly more usable form.

$$G = \frac{2}{\beta} - \frac{F}{\Sigma_{ao} R_o} \tag{9}$$

In practice, instead of using Equation 7 to calculate F one would numerically average the exact rod flux distribution (Eq. 16, HW-33566, loc. cit.).

From the work of H. Neumann[9] one finds

$$F = \frac{\Sigma_{ao} R_o (2-\beta)}{\beta} \tag{10}$$

when both the exit and entering currents are taken to have the diffusion theoretic form. Substitution of Equation 10 into Equation 9 yields G = 1 substantiating our arguments above.

The Exit Thermal Neutron Spectrum from A Hanford Slug - G. W. Stuart

The initial step in our analysis involves calculation of the thermal blackness (i.e., the probability that a thermal neutron incident on a slug will be absorbed) of a natural uranium Hanford (1.69 cm radius) slug vs. energy. This requirement is easily accomplished using the techniques developed[10] in HW-29992 as modified in HW-33566. We have plotted in Figure 3 both the total cross section used to generate the thermal blackness, β, and β itself. A constant scattering cross section of 9 barns is employed.

The obvious remark may now be made that if the thermal neutron spectrum incident on a slug is f(E) then the spectrum of neutrons leaving the slug will be $[1-\beta(E)]\, f(E)$. In Figure 4 we show to arbitrary normalizations an incident 293°K maxwellian flux distribution with its resulting exit flux distribution.

In order to determine the temperature of the exit neutron distribution we fit the β curve in Figure 3 with

---

(9) HW-32128, H. Neumann, Computation of Fuel Rod Disadvantage Factors.

(10) HW-29992, R. W. Woodruff and G. W. Stuart, Calculation of the Thermal Blackness of a Solid Cylindrical Fuel Rod.
HW-33566, G. W. Stuart and R. W. Woodruff, The Successive Generations Method.

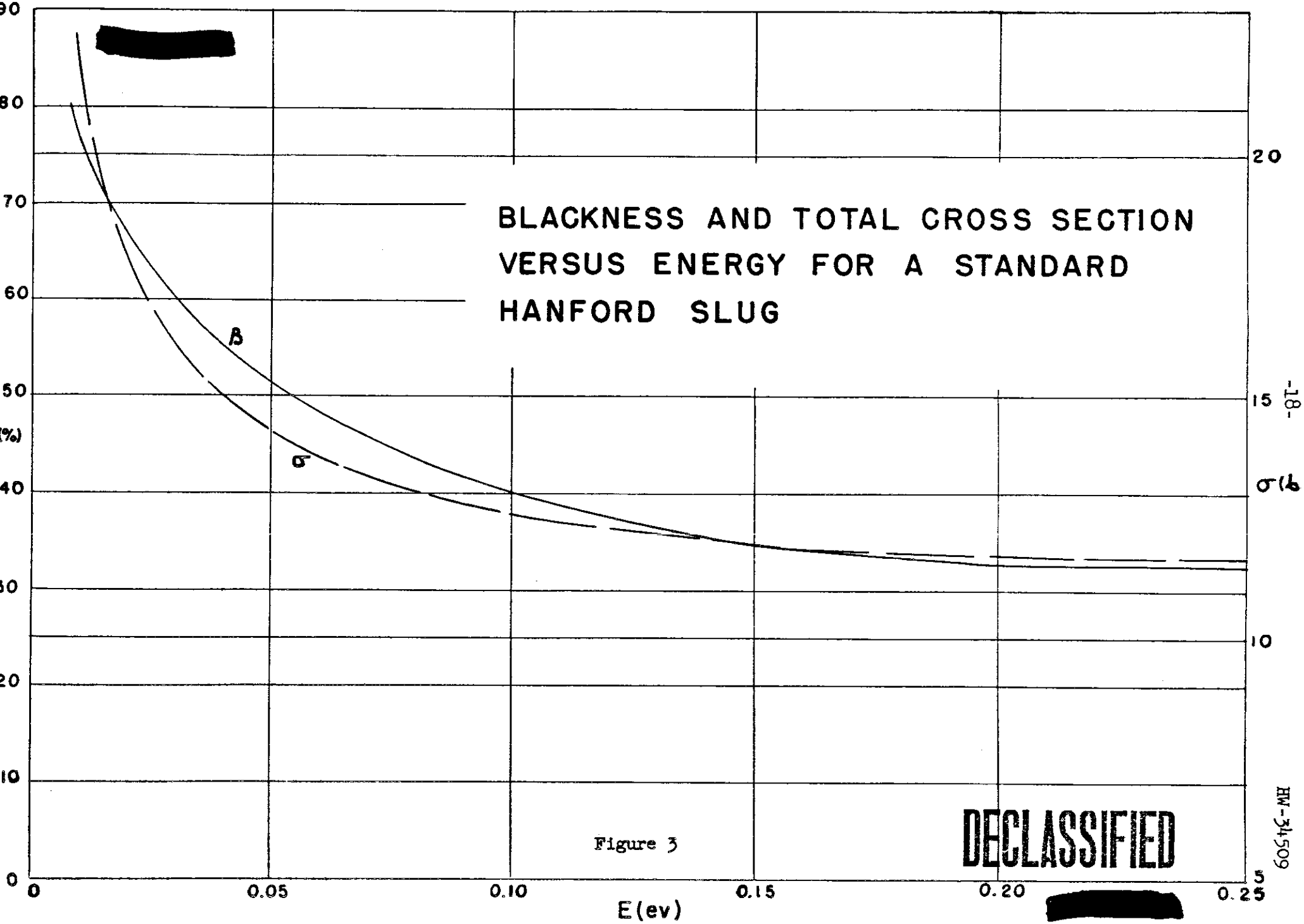

Figure 3

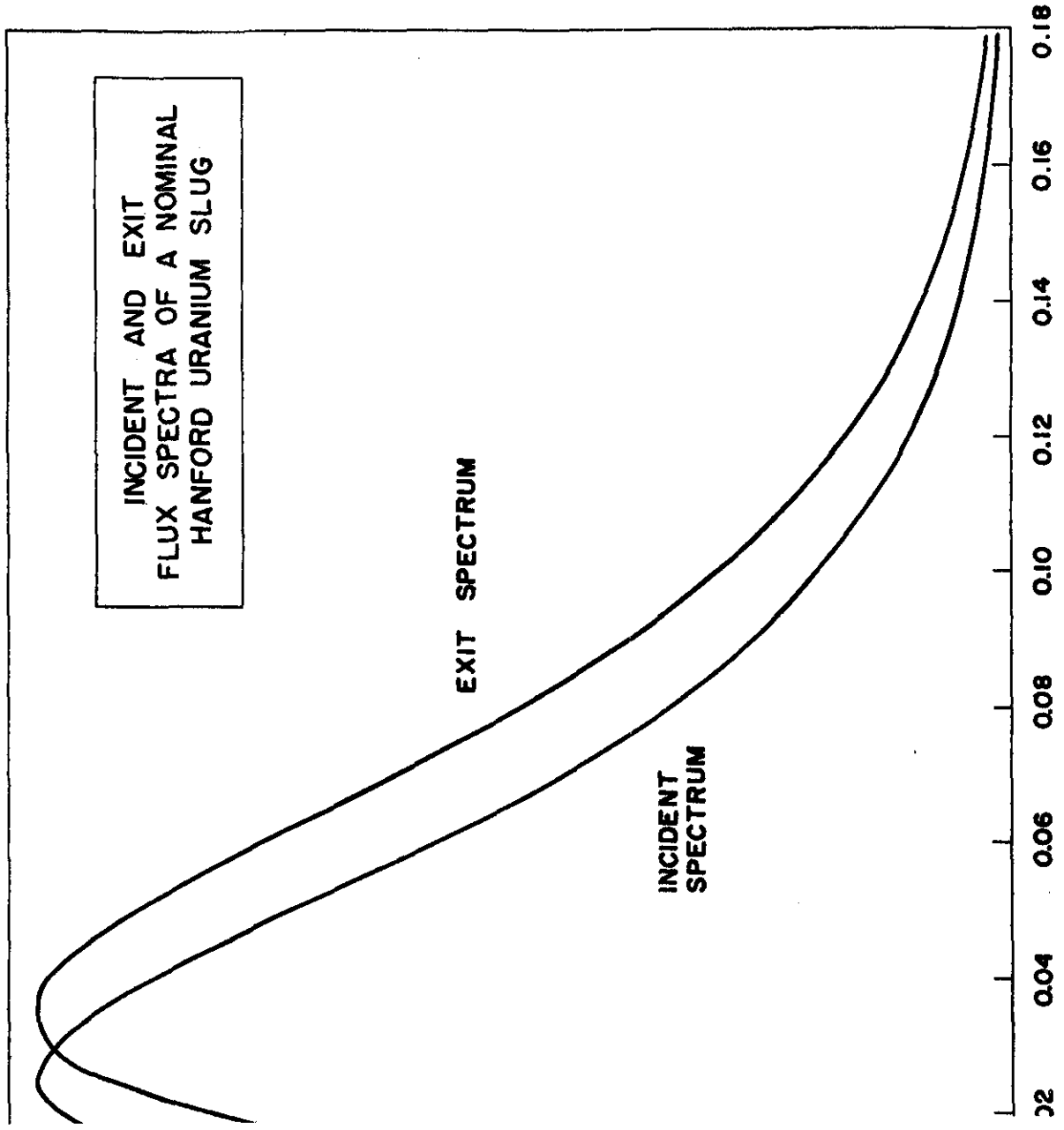

Figure 4

(1) $$\beta = 0.312 + 0.544\, e^{-20.20\, \theta\, x}$$

where $\theta = kT$

$$x = \frac{E}{\theta}$$

The error in this approximation is as follows

E ev.	%
0.010	-1.3
0.015	+0.4
0.020	+1.0
0.040	0.0
0.060	-2.1
0.100	-4.0
0.200	-1.2

One then forms the expression:

(2) $$\langle E \rangle = \theta \frac{\int_0^\infty x^{3/2}\, e^{-x}\, (1-0.312 - 0.544\, e^{-20.20\, x})\, dx}{\int_0^\infty x^{1/2}\, e^{-x}\, (1-0.312 - 0.544\, e^{-20.20\, x})\, dx}$$

$$= 3/2\, \theta \left\{ \frac{0.688 - 0.544\, (1 + 20.20\, \theta)^{-5/2}}{0.688 - 0.544\, (1 + 20.20\, \theta)^{-3/2}} \right\}$$

Inserting $\theta = 0.025$ ev.

(3) $$\langle E \rangle = 3/2\, \theta\, [1.25]$$

revealing a neutron temperature rise of 73°K. Similar results for different energy entering distributions may be obtained by merely inserting the proper θ into Equation 2.

The results exhibited in Equation 3 could only be detected if one employed a directionally sensitive detector. It is also of interest to calculate the experimental results to be expected if one employed a non-directionally sensitive detector. This is obviously

(4) $$\langle E \rangle = 3/2\, \theta \left\{ \frac{1.688 - 0.544\, (1 + 20.20\, \theta)^{-5/2}}{1.688 - 0.544\, (1 + 20.20\, \theta)^{-3/2}} \right\}$$

which is for our case

(5) $$\langle E \rangle = 3/2 \ \theta \left\{1.07\right\}$$

or a temperature rise of 21° K at the slug moderator interface.

The Method of Successive Generations[11] - G. W. Stuart

During the past quarter we have[12] calculated $II_1(1,T)$. This distribution is shown in Figure 5 along with, for comparison, $II_o(1,T)$.

A chart of rod blacknesses was prepared to allow ready reading off of a desired blackness, providing the rod optical path length X and the ratio of rod scattering to rod total cross section Z are given. The range covered is: $0 < X \leqslant 3.0$; $0 < Z \leqslant 0.80$ (0.005). This chart has been incorporated in document HW-34187 to be released into the category Physics and Mathematics.

On Certain Infinite Integrals Involving Bessel Functions - G. M. Muller

In the last Quarterly Report[13] the author mentioned the forthcoming preparation of an unclassified paper describing certain mathematical results discovered in the course of his work on computational methods to be used in connection with the method of successive generations. The author is presenting this paper, entitled as above, at a joint session of the AAAS and the American Mathematical Society at Berkeley, on December 31. The following is the text of the official abstract of the paper: "By the use of a well-known lemma from the theory of hypergeometric functions, it is possible to express various classes of such integrals in terms of elementary, or at least tabulated, functions. As an illustration, it is shown that the integral $\int_0^\infty K_p(t)I_q(tz)t^r dt$ can be expressed in terms of the complete elliptic integrals of the first and the second kind of parameter z, provided the three numbers q, $(q + r \pm p)/2$ are positive integers or zero. A particular case of this result is used in the evaluation of a certain improper integral."

A Note on the Numerical Evaluation of Infinite Integrals - G. M. Muller

Most standard works on numerical analysis do not seem to contain any reference to the following very simple method for evaluating an integral of the form

(1) $$\int_a^\infty f(x)dx, \qquad 0 \leq a < \infty$$

(11) Previous discussions on this subject may be found in reports HW-31351, HW-32349, HW-33384, HW-33566. A reader unfamiliar with this topic is advised to read these articles before attacking the discussion below.

(12) The calculation was performed by the methods discussed by G. M. Muller in HW-33384. Since calculation of $II_n(X,T)$, $n > o$ on the IBM-CPC is an inefficient procedure, extensive tabulation of these distributions awaits the delivery to Hanford of IBM-702 in the late spring.

(13) HW-33384

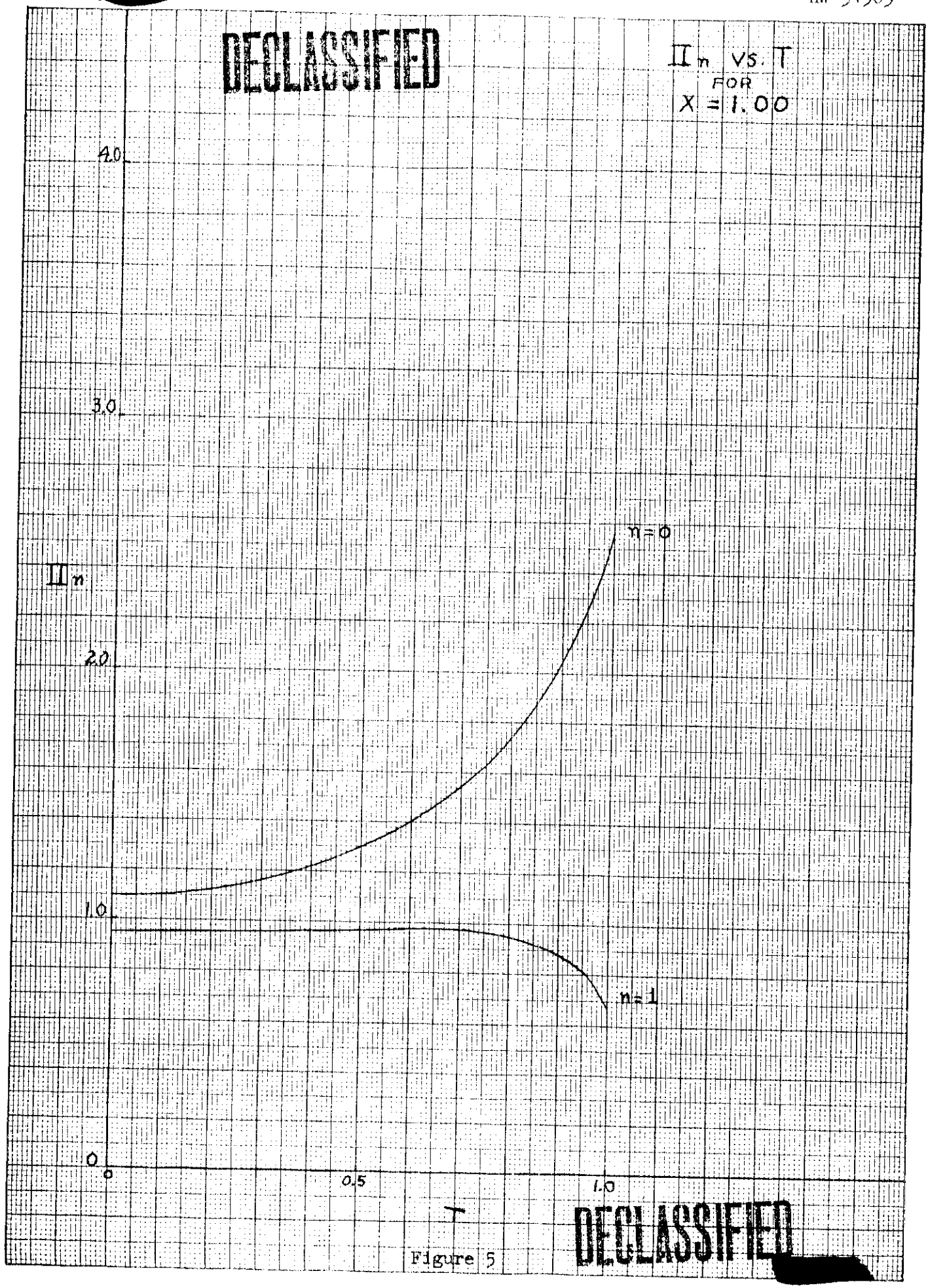

Figure 5

where the integrand is such that, for sufficiently large $x, x^2|f(x)|$ is monotone non-increasing. The usual approach appears to be one in which the computer goes into conference with his conscience to determine a finite number b which may be safely substituted for the upper limit of integration without introducing an appreciable error. The present method, besides eliminating the need for thus searching one's soul, has the advantage of reducing the number of points where f(x) has to be evaluated just in the range whose contribution to the value of (1) is small. It consists merely in making the substitution $t = 1/x$, which leads to

$$(2) \qquad \int_a^{\infty} f(x)dx = \int_0^{1/a} f(1/t)t^{-2}dt.$$

The usefulness of this method can be demonstrated most rapidly by reference to a simple example. Suppose we wish to evaluate the integral $I = \int_1^{\infty} x^{-3}dx$ numerically. Application of (2) yields $I = \int_0^1 xdx$. Using the trapezoidal rule (without any subdivision of the range of integration) produces the result $I = 1/2\ (1 + 0) = 1/2$ with a degree of accuracy which could hardly have been obtained by the direct application of any numerical method to the evaluation of the integral in its original form. Needless to say, this method has been used by the author (with good success) under rather less trivial circumstances.

Buckling Measurements - D. E. Davenport, E. D. Clayton

Buckling measurements in the large (8' x 8') exponential piles, this past quarter, have extended the measurements with the standard Hanford slug (1.36" diameter) to the 10-3/8" lattice spacing and given a measurement of the effect on the buckling of removing a 1/2" diameter core from this slug. The comparison was carried out in the 10-3/8" lattice and will be repeated in the 7" lattice and the 5-3/16" lattice in the future to check the effect over the entire range of interest. The purpose of the measurement of the effect of coring is to investigate the reliability of theoretical calculations of the effect, since some coring seems indicated in future slug designs to improve slug stability at higher exposures.

The results in the 10-3/8" lattice were as follows:

Density of graphite		1.658
Density of uranium		18.75
Volume of aluminum		4.3 cc/cm of cell
Volume of water		2.33 cc/cm of cell
Volume of uranium:	solid slug	8.57 cc/cm of cell
	cored slug	7.41 cc/cm of cell

BUCKLING

	Wet Lattice	Dry Lattice
Solid Slug	25×10^{-6} cm^{-2}	71×10^{-6} cm^{-2}
Cored Slug	11×10^{-6} cm^{-2}	58×10^{-6} cm^{-2}
Difference	14×10^{-6} cm^{-2}	13×10^{-6} cm^{-2}

Although detailed calculations of the theoretically expected differences have not been completed, the measured differences agree well with rough calculations.

Miniature BF_3 Counter

Since time consuming cell traverses seem to call for some simpler, easier to use flux detector than foils, a miniature BF_3 counter was designed which may greatly aid in the measurement in the moderator region. The counter is 1/8" in diameter and 4" long with a 1 mil stainless steel center wire. It is filled to 60 cm pressure of enriched BF_3. The counter has a plateau length of 150 volts with a plateau slope of 5%/100 volts and an operating voltage of about 1500 volts. In the few weeks that it has been in operation, it has shown very good stability and little drift in counting rate. It is presently being used to check the moderator portion of the cell traverse in the 8-3/8" lattice, to investigate its reliability in use.

Neutron Sources - D. E. Davenport, E. D. Clayton

An investigation of possible low cost, readily available neutron sources which would supply 10^7-10^9 neutrons/sec, suggested that two likely possibilities were irradiated compacts of BiF_3 and powdered metal mixtures of Bi and Be. On irradiation Po is produced and the resulting alpha particles from the Po decay yield neutrons from the (α,n) reaction with the fluorine or beryllium. If such a source, with all of the excess bismuth left in the slug, would give a high enough neutron emission, the very expensive separation costs of Po could be avoided. The BiF_3 source has the advantage of being easy to prepare since it has no toxicity problems and requires no mixing since it has a molecular mixture of the target atoms of fluorine with the potential Po atoms. It has the disadvantage of a much lower efficiency of the alpha-target reaction for producing neutrons.

Exposure of two samples of BiF_3 and 3 samples of Bi-Be compacts were carried out. The measured neutron emission of the BiF_3 samples was 60% and 90% of the theoretically calculated emissions from the estimated exposures. Although the 60% figure seems a little low, the calculations could be in error 10-20% because of faulty exposure estimates (the two samples were exposed at different times and locations). The Bi-Be compacts, surprisingly, showed yields of 40-60% of the theoretical value, assuming molecular mixing. Since great care had not been taken to assure very fine particle size nor very uniform mixing, this yield is very good.

These results indicate that it is possible to produce a 1.25" diameter, 4" long BiF_3 source with an initial emission of 10^6 neutrons/sec, while a similar Bi-Be source would have an emission of about 4×10^6 neutrons/sec. A detailed report of the experiment is being prepared.

Fission Resonance Integral in U-235 - D. E. Davenport, E. D. Clayton

Recent discussions about the fraction of the fission events in a graphite moderated reactor which are produced by epicadmium neutrons captured by U-235, suggested that it might be worth while to take a closer look at this problem. The fraction of such fission events occurring will depend upon the ratio of fast to thermal flux. Some measurements here at Hanford had suggested that this number was of the order of 8%, and fission counter measurements made in the 8-3/8" lattice in and near the 1.36" diameter fuel rod seem to confirm this. The cadmium used in this measurement was 20 mils thick, giving a cut-off energy of 0.5-0.8 ev depending somewhat on the definition. However, on comparing this measurement with that obtained with a BF_3 detector, which is a pure 1/v absorber, it was found that the results were very nearly the same.

To get a more quantitative measure of the fission resonance integral above cadmium cut-off, the integral was measured using a method suggested in the literature(14),(15) and the fission counter as the detector. The activity of a cadmium-covered detector is given by

$$A_{Cd} \sim \frac{q\lambda}{\zeta} \int_0^{2\ \text{Mev}} T(E)\sigma(E)\,\frac{dE}{E} \tag{1}$$

where T(E) is the transmission factor for the cadmium cover. The thermal activity, or activity due to those neutrons which are absorbed by the cadmium, is given by

$$A_{th} = \text{Bare activity} - \text{Cd covered activity} \sim nv\,\bar{\sigma}$$

where $\bar{\sigma}$ is the average cross section for neutrons absorbed by the cadmium cover or, essentially, the average cross section for thermal neutrons. The cadmium ratio is the ratio of the bare detector activity to that of the cadmium-covered detector. Therefore

$$C.R. - 1 = \frac{A_{th}}{A_{Cd}} .$$

(14) Anderson, Fermi, Wattenberg, Weil and Zinn, Method for Measuring Neutron Absorption Cross Sections by the Effect on the Reactivity of a Chain Reacting Pile, Phys. Rev., Vol. 72, July 1947.

(15) Harris, Muehlhause, and Thomas, Low Energy Neutron Resonance Scattering and Absorption, Phys. Rev., Vol. 79, July 1, 1950.

In terms of the cadmium ratio, the usual relationship for the resonance integral is then given[14] from the above relations as

$$(2) \qquad \int_{Cd} \sigma \frac{dE}{E} = \frac{nv\, \zeta\, \bar{\sigma}}{q\, \lambda\, (C.R. - 1)}$$

where the transmission factor in the resonance integral has been removed and replaced by changing the lower limits of integration from zero to cadmium cut-off energy--the rather nebulous quantity which has only this equivalence for a definition. If the quantity $\frac{nv}{q}$ is known, then the resonance integral above the cadmium cut-off is determined.

From indium foil standardizations carried out in the Hanford Standard Pile[16] this quantity is given by

$$\frac{nv}{q} = 48.26\ (C.R. - 1.08)$$

for the standardized foils.

The fission chamber used in the measurements was 1-3/4" long and 5/16" in diameter containing a total of 1.94 mg of uranium which was 95.7% U-235. The center wire was 2 mils in diameter, and the counter was filled to a pressure of 1 atmosphere of argon. The thickness of the uranium on the platinum foil which lined the inside circumference of the chamber was 0.33 mg/cm^2. This layer was sufficiently thin so that there was essentially no self shielding of the foil for resonance neutrons. This chamber possessed a good discriminator plateau (about 18% change in the counting rate for a discriminator change from 35 to 100 volts on the Atomic Instruments 204 C linear amplifier).

The measurements were taken in the small (4' x 4') exponential pile with the 8-3/8" wet lattice loaded with the standard Hanford slugs. The cadmium ratio was measured at the corner of the lattice cell where its value would be the highest. The cadmium ratio for the standardized indium foils was found to be 7.98, therefore

$$\frac{nv}{q} = 48.26\ (7.98 - 1.08) = 333 \text{ cm.}$$

The cadmium ratio for the small fission chamber was 35.5. The fission resonance integral above the cadmium cuf-off (20 mil cadmium) is then

$$\int_{Cd} \sigma_f \frac{dE}{E} = \frac{333\, \bar{\sigma}_f\, \zeta}{\lambda\, (34.5)}$$

(16) HW-26207, Davenport, Lynn, Richey, The Standardization of Gold and Indium Foils.

 [redacted]

Taking

$$\overline{\sigma_f} = \frac{0.98\ (580)}{1.128} = 504 \text{ barns}$$

$$\zeta = 0.158$$

$$\lambda = 2.73 \text{ cm.}$$

then

$$\int_{Cd} \sigma_f \frac{dE}{E} = 281 \text{ barns}$$

This integral gives the total fission cross section above cadmium cut-off and includes the 1/v absorption. If the material had a pure 1/v cross section with the same average thermal cross section, theoretical calculations show that its epicadmium cross section would be 276 barns. The appropriate value for the epicadmium cut-off is somewhat uncertain but is probably about 0.6 ev for U-235 covered with 20 mil cadmium. Owing to the uncertainty in the appropriate cadmium cut-off and other possible systematic errors, the uncertainty in the above integral is probably of the order of 10%.

Numerical integration of the fission cross section from 0.17 ev, the approximate joining energy for the Maxwellian and $\frac{1}{E}$ tail, to 0.6 ev indicates that this portion contributes an additional 190 barns of which only 36 barns are added in the region between 0.4-0.6 ev. This indicates the relative insensitivity of the above result to the exact value of the cadmium cut-off which is assumed. Additional details and the results of further measurements will be given in a separate report.

U-233 Concentration and Burnout in Thorium Metallurgical Samples - R. W. Woodruff and G. W. Stuart

At the request of the Metallurgy Research Sub-Section we have calculated the U-233 concentration and burnout in thorium metallurgical samples where burnout is defined as the ratio of the number of U-233 nuclei which disappear during the irradiation to the number which remain at the end of the irradiation. Our results are presented in HW-34228.

Relative Conversion Ratio Measurement - H. W. Lefevre

Two foil irradiations were made during the startup of the KW reactor. These irradiated foils will give a comparison of the conversion ratic in the 7-1/2" wet lattice with the 8-3/8" lattice, and with other lattices to be tested in the prototype LTR. A production test has been written which will allow use of the Hanford Test Pile as a standard irradiation facility for relating data obtained over a long time interval.

[redacted]

NUCLEAR PHYSICS

Neutron Spectrometer Facilities - B. R. Leonard,Jr., E. J. Seppi, W. J. Friesen

I. Fast Neutron Detector Development

Some development work has been done on a fast neutron detector for possible use in measurements of η and ν. The fast neutron detector investigated was the Hornyak button,(17) which consists of a homogeneous mixture of molded ZnS (Ag) phosphor and lucite. The primary mechanism of fast neutron detection is the detection of recoil protons in lucite by means of ZnS(Ag) scintillations. Eight buttons in the shape of 2-inch diameter right cylinders were prepared by oven heating a mixture of ZnS (Ag), with an average grain size of 8 microns, and lucite molding powder in a mold to a temperature of 200° C and molding under a sustained pressure of 3500 lbs/in^2. This procedure produced a clear bubble-free lucite button when no ZnS (Ag) was added to the lucite. The amounts of ZnS (Ag) and lucite used in the buttons are listed in Table I. The reflector and light shielding for the buttons consisted of 5.4 mg/cm^2 aluminum foil and one layer of scotch black and electrical tape. Clear mineral oil was used for an optical coupling between the buttons and an RCA 6342 photomultiplier tube.

To determine the relative fast neutron efficiencies of the buttons, the detector was shielded from slow neutrons with 0.040 inches of cadmium and placed directly behind a U-235 disk in the 0.1 ev diffracted neutron beam of the crystal spectrometer. With the gain and discriminator bias held constant, the counting rate associated with each of the buttons tested was compared with the counting rate of a thin boron ionization chamber which monitored the slow neutron flux incident on the U-235 source disk. The efficiencies of the buttons tested at an arbitrary setting of gain and bias are listed in Table I.

For the particular grain sizes of the materials used in the buttons, the optimum areal density of ZnS (Ag) is 0.20 gm/cm^2 or less. The results also indicate that for the source geometry used, a button somewhat thinner than Button 1 and containing around 0.20 gm/cm^2 of ZnS may have a higher detector efficiency than the buttons tested.

Figure 6 shows the results of an investigation of the efficiencies of Button 1 for detection of fast neutrons and gamma rays as a function of discriminator bias. Curve A shows the relative counting rate as a function of discriminator bias of the fast neutron detector counting events from a U-235 target using a 0.040-inch cadmium cover to shield the button from slow neutrons. Curve B shows the relative counting rate as a function of discriminator bias of the fast neutron detector with the U-235 source disk removed from the beam. Both curves have been normalized so that the ordinate gives the efficiency for fast neutron detection in a 50% geometry. A fast neutron component in the slow neutron beam is seen as a change in the slope of Curve B at biases above 10 volts. The contribution to the

(17) Hornyak, W. F., A Fast Neutron Detector, Review of Scientific Instruments, June 1952, p. 264

FIGURE 6 FAST NEUTRON DETECTOR EFFICIENCY

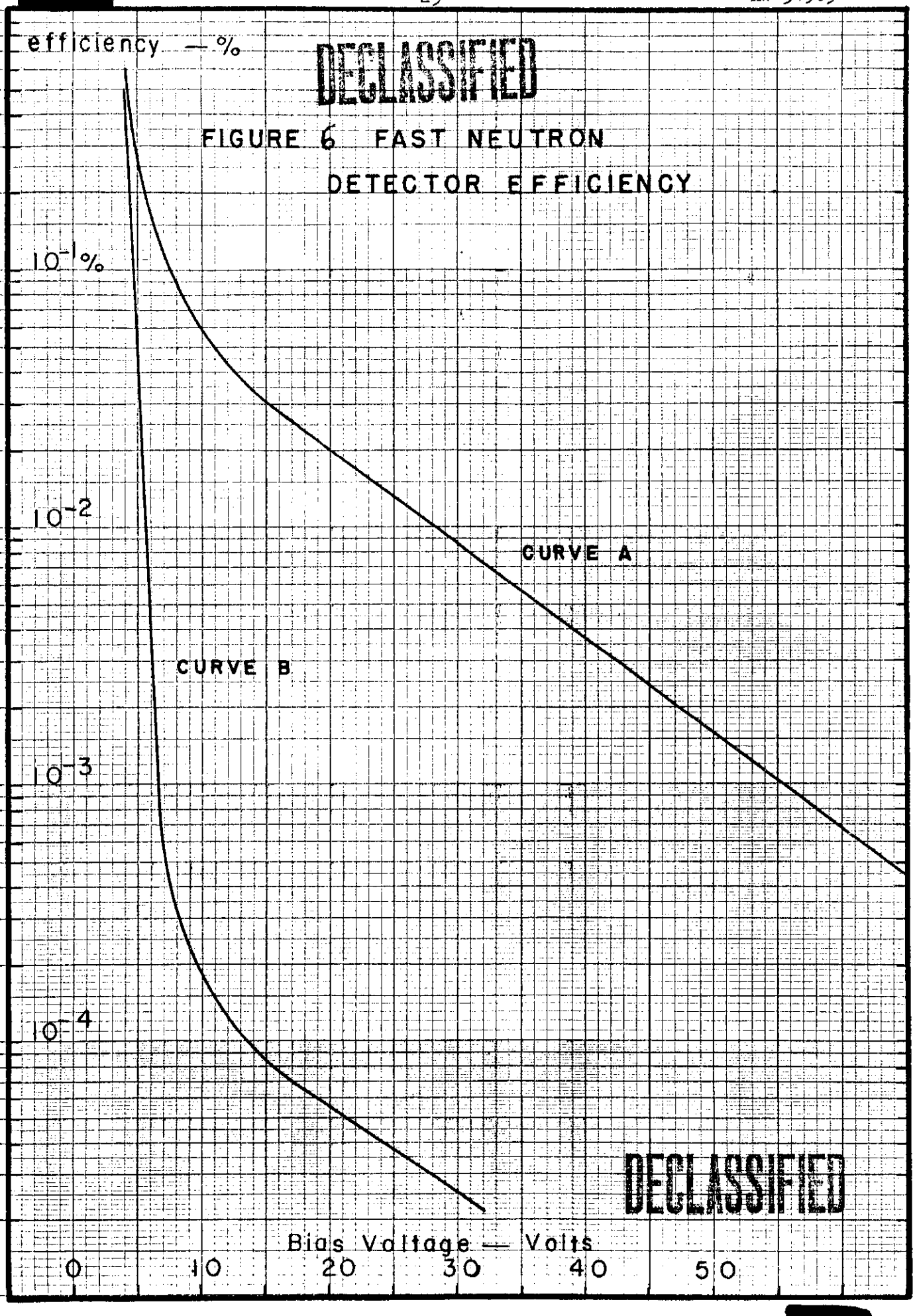

counting rate of Curve A at a 10-volt bias due to gamma rays and slow neutrons is less than 0.01%.

Figure 7 shows the relative variation with time of the observed efficiency of the fast neutron detector while counting a constant source. The observed change in efficiency with time is probably due to voltage drifts in the electronic components. The slope of the efficiency versus discriminator bias at a bias of 12 volts is about 12 per cent per volt. The slope of the efficiency versus photomultiplier tube voltage is about 3 per cent per volt at the operating voltage of 900 volts. An investigation of detector efficiency as a function of counting rate was made by inserting a filter into the diffracted beam to vary the incident neutron flux. The efficiency increased by less than one per cent for a change in counting rate from 3×10^3 to 100×10^3 counts per minute.

TABLE I

Button Data

Button No.	11	6	4	7	1	10	8	9
Length of 2" Diameter Cylinder (inches)	1.5	1.5	1.5	1.5	0.48	0.75	0.75	0.75
ZnS(Ag) (gm/cm^2)	0.01	0.20	0.30	0.40	0.115	0.20	0.30	0.40
Lucite (gm/cm^2)	4.4	4.4	4.4	4.4	1.4	2.2	2.2	2.2
Fast Neutron Efficiency x 10^4 (at 12 v. disc.bias)	0.21	0.45	0.39	0.46	4.2	2.3	2.8	2.5

II. An Experiment to Investigate the Relative Variation in ν with Neutron Energy.

The feasibility of an experiment for measuring the relative variation in ν, the average number of fast neutrons emitted during the slow neutron fission of U-235, as a function of incident neutron energy has been investigated. The experiment consists of using a Hornyak button to detect fast neutrons from U-235 fissions caused by monoenergetic neutrons from the crystal spectrometer. The observed counting rate is proportional to ν and to the fission rate of the target. By using a fission fragment ionization chamber with a thin U-235 foil as the neutron detector, to obtain a number proportional to the fission rate, the relative variation in ν with incident slow neutron energy can be observed. At present the "best value" which has been obtained for the ratio of ν for 0.29 ev neutrons to ν for 0.10 ev neutrons is 1.036 ± 0.010. Where the quoted error is the accumulated statistical error of the measurements involved and does not contain any contribution due to instrumental and systematic errors.

Figure 7

A relation between the observed counting rates and ν can be obtained as follows: If the fast neutron detector efficiency is low enough ($\epsilon \lesssim \sim 1\%$) to insure that a negligible number of counts are lost due to coincidence detection of fast neutrons from a single fission, the counting rate of the fast neutrons detector will be given by

$$R = \nu N \sigma_f \epsilon \int_0^L \phi \, dx \tag{1}$$

where N is the atomic density of the target, σ_f is the fission cross section of the target material, ϵ is the overall efficiency of the fast neutron detector, L is the thickness of the target, and ϕ is the effective slow neutron flux distribution through the target. Neglecting the small increase in the effective neutron flux due to the scattered neutrons, the flux distribution is given by

$$\phi = \phi_o e^{-N x (\sigma_s + \sigma_a)} \tag{2}$$

where σ_a and σ_s are respectively the absorption and scattering cross section of the target materiald and ϕ_o is the incident slow neutron flux. Substituting Equation 2 into Equation 1 and dividing both sides by the counting rate of the fission fragment ionization counter gives

$$\frac{R}{R_f} = \frac{\nu N \sigma_f \epsilon \phi_o \int_0^L e^{-N x (\sigma_a + \sigma_s)} dx}{\kappa \sigma_f \phi_o} \tag{3}$$

where κ is a constant.

Integrating and solving for ν gives

$$\nu = \frac{\kappa R (\sigma_a + \sigma_s)}{\epsilon R_f \left[1 - e^{-NL(\sigma_a + \sigma_s)}\right]} \tag{4}$$

If $e^{-NL(\sigma_a + \sigma_s)}$, the slow neutron transmission of the fast neutron source, is greater than 90%, Equation 4 can be approximated to within 0.5% by

$$\nu = \frac{\kappa R}{\epsilon NL R_f} \tag{5}$$

If $e^{-NL(\sigma_a + \sigma_s)}$ is between 90% and 70%, Equation 4 can be approximated to within 0.5% by

$$\nu = \frac{\kappa R}{\epsilon NL R_f T^{1/2}} \tag{6}$$

where T is the slow neutron transmission of the target.

To determine the practical feasibility of this experiment, a U-235 source disk for which the Equation 6 is valid, was used to measure the relative change in ν between the slow neutron energies 0.10 and 0.29 ev. The counting rates of the fast neutron detector and the ionization detector were determined at spectrometer settings corresponding to these two energies. The background contribution to these counting rates was obtained by rotating the spectrometer crystal two and one-half degrees from the Bragg angle. The transmission of the disk for neutrons of 0.29 and 0.10 ev were measured and found to be 0.781 ± 0.003 and 0.739 ± 0.005 giving 0.973 ± 0.004 for $\left[\frac{T(0.10)}{T(0.29)}\right]^{1/2}$. According to Equation 6, the ratio of ν at these two neutron energies is given in terms of the observed counting rates by

$$(7) \qquad \frac{\nu\ (0.29)}{\nu\ (0.10)} = 0.973\ \frac{R(0.29)\ R_f(0.10)}{R(0.10)\ R_f(0.29)}$$

The sources for instrumental and systematic error which have been given a preliminary investigation are:

1) The instability of the fast neutron detector used. This instability has been previously discussed. To prevent error due to the time instability of the detector, the ratio $\nu(0.29)/\nu(0.10)$ was measured in a short total counting time. To reduce the statistical error, the measurements were repeated several times and then averaged. Using this method, the measurements of the ratio $\nu(0.29)/\nu(0.10)$ under a given set of experimental conditions could be repeated to within their predicted statistical accuracy.

   The value of $\nu(0.29)/\nu(0.10)$ as determined above may also have an error in it due to a possible change in fast neutron detection efficiency with counting has been previously discussed. This effect tends to make the observed value of $\nu(0.29)/\nu(0.10)$ lower (by less than 1%) than the true value.

2) The error due to second order slow neutrons. The preliminary measurements of $\nu(0.29)/\nu(0.10)$ were not corrected for second order effects. Measurements of the magnitude of this correction have been made using standard filter techniques. These preliminary measurements indicate that the correct value of $\nu(0.29)/\nu(0.10)$ can be obtained from the observed uncorrected value by multiplying by 1.01 ± 0.01.

3) The constancy of fast neutron detection efficiency with spectrometer position. The derivation of Equation 7 depends on the constancy of ϵ. To investigate the possibility of a change in ϵ due to a change in the incident slow neutron distribution with spectrometer angular position, measurements were made for incident neutron beams collimated to 1-1/4", 7/8" and 1/2" diameter. Table II summarizes values of $\nu(0.29)/\nu(0.10)$ which have been obtained using various slow neutron beam diameters and various discriminator biases. The table shows that data obtained using a 1-1/4" diameter slow neutron beam were somewhat higher than data obtained using 7/8" and 1/2" diameter slow neutron beams, thus indicating

some inconstancy of ϵ with spectrometer setting. This effect should not be as great for slow neutron beams of smaller diameters; data obtained using a 7/8" diameter slow neutron beam as compared to that obtained using a 1/2" diameter slow neutron beam are inconclusive and further measurements need to be made. The best value of $\nu(0.29)/\nu(0.10)$ that has been obtained is 1.036 ± 0.010. This value was obtained by taking a weighted average of measurements using 7/8" and 1/2" collimation and correcting the results for second order.

TABLE II

A List of Values for the Ratio $\frac{\nu(0.29)}{\nu(0.10}$ Which Have Been Obtained Using Various Incident Slow Neutron Beam Diameters and Various Discriminator Biases*

Bias	1-1/4" Diameter Beam	7/8" Diameter Beam	1/2" Diameter Beam
10 Volts	1.063 ± 0.009 1.055 ± 0.008 1.058 ± 0.006	1.018 ± 0.007	
12		1.034 ± 0.006	1.031 ± 0.01
15	1.053 ± 0.002		
20	1.043 ± 0.01		1.018 ± 0.009

* The errors quoted in this table are due to the accumulation of statistical errors in the counting rates involved in the calculation of $\nu(0.29)/\nu(0.10)$ using Equation 7.

Th-232 Effective Absorption Cross Section - R. E. Peterson

A 4π proportional counter to be utilized in absolute counting of Th-233 β activity has been constructed and placed in operation. In order to determine how well the counter operates, several calibrated Co-60 sources have been made up on thin film for absolute counting. Since the Co-60 β is much less energetic than the Th-233 β, (0.32 Mev as compared with 1.23 Mev) little difficulty should be encountered in counting Th-233 if Co-60 can be counted absolutely with this instrument.

Consideration is now being given to preparation of a sample of Th-232 for exposure. Thorium nitrate appears to be the most convenient compound for deposition on thin films since it is water soluble. However, it is of uncertain hydration and this must be determined prior to weighing out a sample for irradiation. A direct method for establishing the degree of hydration is to ignite a weighed sample to thorium oxide and weigh the oxide.

C-12 Absorption Cross-Section Measurement - R. E. Peterson

Mass analysis of the LiI flux monitor has been completed by Dr. R. J. Hayden of Argonne National Laboratory. The results of his analysis are as follows:

$$\frac{Li^7}{Li^6} \text{ unirradiated} = 12.24, \qquad \frac{Li^7}{Li^6} \text{ irradiated} = 95.1$$

The ratio of Li^7 to Li^6 in natural Li (R_{oLi}) is given as 12.5 so that the estimated error in the above ratios is about 2%.

Upon obtaining the ratio of Li^7 to Li^6 in the irradiated material (R_{Li}), the average thermal neutron flux ($\bar{\phi}_{Li}$) incident upon it is given by the relationship(18)

$$R_{Li} = R_{oLi}\, e^{(\sigma_6-\sigma_7)\bar{\phi}_{Li}NT} + \frac{\sigma_6}{\sigma_7-\sigma_6}\left[1 - e^{(\sigma_6-\sigma_7)\bar{\phi}_{Li}NT}\right]$$

where σ_6 and σ_7 are the Li^6 and Li^7 cross sections averaged over a Maxwellian distribution

N is the number of irradiation cycles

T is the length of each cycle.

Solution of the equation for $\bar{\phi}_{Li}$ yields a value of 2.84×10^{14} $n/cm^{-2}/sec^{-1}$. This value, corrected for variation of flux with vertical position in the stringer, should then give the "1/v" flux incident upon the primary cobalt monitor. However, the vertical flux traverse indicates a position factor which is too large on the basis of the absolute activities of both primary and secondary cobalt monitors. The cobalt-aluminum wire will be scanned once again in an attempt to remove this discrepancy.

Radio Assay for the Neptunium-239 Activation Cross-Section Measurement - H. W. Lefevre

In connection with an experiment being conducted by E. M. Kinderman, an absolute analysis of the Neptunium-240 produced by an irradiation of freshly separated Np-239 will be made. This will be done by comparing gamma activities of the neptunium sample with a calibrated standard. Since at this time we do not know which of two reported states of Np-240 will be produced by neutron capture in Np-239, standards have been prepared to allow us to make an assay of either. The gammas which will be used for comparison are of energy greater than 1 Mev which allows use of lead filters to remove the lower energy Np-239 gammas.

(18) HW-29569, Analysis of Errors to be Expected in Measuring the Neutron Absorption Cross Section of C^{12}, E. J. Seppi

Scintillation Counting Techniques - H. W. Lefevre

Six RCA 6342 photomultipliers have been tested for resolution, gain stability versus counting rate, and afterpulsing with a Harshaw-canned NaI crystal. The crystal was nonuniform, giving an unsymmetrical photopeak for Cs-137, the high energy side being steeper. With this crystal the resolution of all six tubes was between 9.0 and 9.5% full width at half maximum. A good crystal mounted directly on the face of one tube gave 8% resolution.

None of these tubes showed any gain drift with counting rate such as the Dumont 6292 tubes in use here have shown. Afterpulsing was serious in three tubes when the overall voltage exceeded 1000 volts. This afterpulsing combined with a lower gain may make use of the Dumont 6292 necessary for some applications even though the stability is poorer. For most conventional applications, the advantage gained from increased stability of the 6342 will offset the slightly better resolution which may be obtained from a selected 6292.

The Plutonium Fission Cross Section f Factor - G. W. Stuart

The Pu-239 fission cross section f factor has been recalculated on the Hanford IBM-CPC equipment using the standard definition

$$(1) \qquad f = \frac{\int_0^\infty \frac{E}{(kT)^2} e^{-E/kT} \sigma(E) dE}{\sqrt{\frac{\pi}{2}}\, \sigma(kT)}$$

The resulting curve agrees exactly with that presented in BNL-250 up to E = 0.060 ev. At that energy a point of inflexion appears in our curve and it turns below that published by Brookhaven. The calculation was carried out to E = 0.100 ev, i.e., T = 1172 °K.

A document, HW-34162, has been issued containing the detailed results.

Thermal Test Reactor - W. P. Stinson

I. Instrumentation

The total time required for the safety rods of the TTR to fall completely into the reactor after a scram signal is received has been measured for two different types of tripping mechanism.

A block diagram of a level trip channel of the TTR is shown in Figure 8.

FIGURE 8

Block Diagram of a Level Trip Channel of the TTR

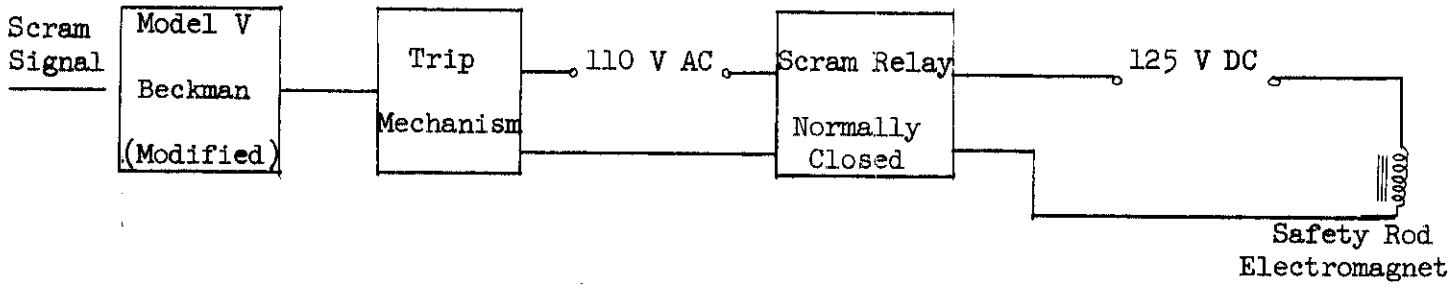

The Model V Beckman DC Amplifier was modified by changing a 3,000 μf condenser (C-12 on circuit diagram) to 1,000 μf as described in GEL-0219. This decreased the total time measured by a factor of two for some of the scale ranges.

For one set of measurements the tripping mechanism was a Model 705 Sensitrol Relay. The other tripping mechanism was a trip circuit with a speed of operation of about 0.02 seconds. This circuit was designed and built by D. C. Pound. The tripping mechanisms were connected to the Beckman recorder output terminals, and were set to actuate when the voltage at these terminals was equivalent to a full scale deflection of the meter.

The time measured was that from the instant a current step-function of twice the magnitude necessary for full scale deflection of the meter on the Beckman was applied to the input of the Beckman to that where the safety rods operated the "in" limit switch. The drop time of the safety rods was 0.433 seconds. The results are tabulated in Table III.

Table III

The Operating Time of a Level Trip Channel of the TTR in Seconds Using a Modified Model V Beckman

Beckman Scale	Sensitrol Relay	Trip Circuit
3×10^{-7}	0.82	0.60
10×10^{-8}	0.88	0.65
3×10^{-8}	0.95	0.65
10×10^{-9}	1.03	0.68
3×10^{-9}	0.87	0.63
10×10^{-10}	1.00	0.70
3×10^{-10}	1.03	0.78
10×10^{-11}	1.13	0.83
3×10^{-11}	0.85	0.55
10×10^{-12}	0.90	----
3×10^{-12}	1.03	----
10×10^{-13}	1.02	0.68

II. Graphite Fabrication

All of the graphite blocks for the TTR have been machined from 4-1/4" to 4-3/16" square. The pieces directly adjacent to the core have been re-machined to close tolerances with high quality graphite.

IRRADIATION PHYSICS

Changes in the Thermal Properties of Solids Caused by Impurities - G. W. Stuart

A calculation has recently been published by Dugdale and MacDonald[19] investigating the thermal properties of a linear chain of identical particles. These authors assumed interatomic forces to be generated by the Morse potential. They then formulated and analytically evaluated the partition function of such a system under constant force. This final step involved some mathematical manipulation which included the discard of small order terms. Proceeding through the established methods of statistical thermodynamics, these authors were then able to present expansions for the specific heats, the compressability and the coefficient of thermal expansion (plus other quantities which we shall not concern ourselves with here). The authors then compared their results with experiment and commented on the strength and weaknesses of the linear approximation.

We have found that the results of Dugdale and MacDonald may be simply extended to the situation where impurity atoms are included in the linear chain. It is clear that relations expressing the changes of the thermal properties of solids with impurity content would be valuable in studying the stability of nuclear fuels as a function of fission product content. It turns out that the exact positioning of impurity atoms within the chain does not enter into our results, only the total number of such impurities matters, producing a great simplification.

We proceed as follows: Upon introducing M/2 similar impurity atoms which displace original lattice atoms, Equation D.1 becomes

$$(1) \qquad V = \sum_{n=1}^{N-M} D(e^{-a(y_n - y_{n-1})} - 1)^2 + \sum_{m=1}^{M} D_1(e^{-a_1(y_m - y_{m-1})} - 1)^2$$

where now a, D are the Morse potential parameters between two similar atoms of the pure chain while a_1, D_1 are the Morse potential parameters between an impurity atom and an atom of the original chain. We have assumed in Equation 1 that impurity atoms are present in such low concentrations that it would be improbable that two of them should occupy adjacent positions in the chain.

The partition function for the impure chain is then found, from purely formal manipulation, to be the product of two terms each having the form Equation D.8, one involving the parameters a, D, N-M, and the second a_1, D_1, M. From this partition function we may calculate the thermal behavior of a linear chain

(19) J. S. Dugdale and D. K. C. MacDonald, Phys. Rev., 96, 57 (1954). The notation of these authors will be used throughout. Their equations will be prefixed with D.

lattice containing impurities. Used in connection with Equation D.10 through Equation D.13, one can obtain the fractional changes in the thermal properties of such lattices that are due to impurity content. Thus we have for the compressibility, C:

$$(2) \qquad \frac{\Delta C}{C} = \frac{a^2 D M}{a_1^2 D_1 N}\left(\frac{\frac{1}{2}+\frac{11}{8}\frac{kT}{D_1}+\cdots-\frac{3}{4}\frac{P}{a_1 D_1}\cdots}{\frac{1}{2}+\frac{11}{8}\frac{kT}{D}+\cdots-\frac{3}{4}\frac{P}{aD}\cdots}-1\right),$$

for the thermal expansion, ρ,

$$(3) \qquad \frac{\Delta\rho}{\rho} = \frac{a D M}{a_1 D_1 N}\left(\frac{\frac{3}{4}+\frac{19}{8}\frac{kT}{D_1}+\cdots-\frac{11}{8}\frac{P}{a_1 D_1}+\cdots.}{\frac{3}{4}+\frac{19}{8}\frac{kT}{D}+\cdots-\frac{11}{8}\frac{P}{a\,D}+\cdots.}-1\right),$$

for the specific heat at constant force (pressure), C_p,

$$(4) \qquad \frac{\Delta C_p}{C_p} = \frac{M}{N}\left(\frac{1+\frac{kT}{D_1}+\frac{15}{4}\left(\frac{kT}{D_1}\right)^2+\cdots-\frac{P}{a_1 D_1}\left(\frac{19}{8}\frac{kT}{D_1}+\cdots.\right)+\cdots.}{1+\frac{kT}{D}+\frac{15}{4}\left(\frac{kT}{D}\right)^2+\cdots-\frac{P}{a\,D}\left(\frac{19}{8}\frac{kT}{D}+\cdots.\right)+\cdots.}-1\right),$$

and for the specific heat at constant length (volume), C_ℓ,

$$(5) \qquad \frac{\Delta C_\ell}{C_\ell}_{(P=0)} = \frac{M}{N}\left(\frac{1-\frac{1}{8}\frac{kT}{D_1}-\frac{9}{32}\left(\frac{kT}{D_1}\right)^2-\cdots.}{1-\frac{1}{8}\frac{kT}{D}-\frac{9}{32}\left(\frac{kT}{D}\right)^2-\cdots.}-1\right).$$

Despite the crudeness of the linear model, it is felt that Equations 2 through 5 give some indication of the actual behavior of a solid containing impurities. Note that although a and D are extensively tabulated for metals, we must still determine a_1 and D_1 through quantum mechanical methods. Indeed, all that we have achieved in this note is to ready a framework within which a_1 and D_1 will be used.

It is planned to extend this calculation by assuming a two dimensional lattice to replace the linear model. The inclusion of interstitial atoms will also be considered.

PHYSICS PROBLEMS CONNECTED WITH PLANT OPERATIONS

Critical Mass Problems - D. D. Lanning

The plutonium solutions used in the Separations Plants in the past have been in the concentration range of 0 to 150 g/l or have been handled in batch sizes, such that the experimental critical mass data taken at the P-11 project(20) could be applied to the criticality hazards which arose in the handling of these solutions. Recently, however, certain Separations Plants such as Purex and Recuplex have been designed to have continuous flow processes by the use of vessels whose geometric configuration causes enough neutron leakage to keep any plutonium solution from ever approaching criticality in these vessels. Actual experiments to determine these vessel sizes have never been performed. These experiments were not done at P-11 because of the chemistry of plutonium which is involved. In order to obtain the high concentrations of plutonium desired, the nitric acid normality had to be rather high to keep the plutonium in solution. The effect of the nitrate from the HNO_3 and plutonium nitrate was to displace the hydrogen moderator and add the more neutron absorbing nitrogen. Hence, good clean critical experiments could not be performed with plutonium in solution. No experiments were considered for using precipitated plutonium in water slurries. The present vessel sizes as designed for these plants are based on extrapolation of the data taken at the P-11 Project. This extrapolation gives about 8.1 inches as the "always safe" cylinder diameter of a bare cylinder containing Pu-239 in water. At the time these extrapolations were first made it was realized that, for the experimental data, the major portion of the fissions were initiated by neutrons of thermal energy and in the region into which the data were extrapolated the major portion of the fissions would be caused by neutrons of energies considerably greater than thermal. However, in the discussion of this point it was decided that the moderator displacement caused by the increased fuel concentration would probably make these extrapolations conservative. Recently, G. Safanov(21) made a multi-group diffusion theory calculation in which some account could be taken for the variation of the fission and capture cross sections of Pu-239 and the water cross sections with energy. This calculation was fitted by some cross-section juggling to the P-11 data and to metal critical mass data for the case of no moderator in the critical assembly. The intermediate cases could then be calculated giving a curve of critical mass versus bare sphere radius for the case of Pu-239 metal mixed with water and on this curve the H_2O/Pu-239 mole ratio was noted for various points. This curve is not the curve of interest to the Separation Plant problem since it predicts a diameter of a cylinder which is safe from any chain reaction of plutonium to be about 3 inches for a bare cylinder of Pu-239 metal whose density is 15.8 g/cc. The worst case considered in Separations Plants using plutonium solutions is the case of the water slurry of a plutonium precipitate. For this case, if all of the water is driven off of the precipitate it is felt that the cake would not have a density greater than about 3.5 g/cc. G. M. Muller has

(20) Kruesi, F. E., Erkman, J. O., Lanning, D. D., Critical Mass of Plutonium Solutions, HW-24514

(21) Safanov, G., Survey of Reacting Mixtures Employing U-235, Pu-239, and U-233 for Fuel and H_2O, D_2O, C, BeO for Moderator, R-259

shown by purely dimensional arguments that the critical radius of infinitely high cylinders varies inversely as the density of the material in the reactor.

Hence, for the dry slurry case $D \simeq 3 \frac{15.8}{3.5} = 13.5$ inches for the "always safe" diameter of a bare cylinder containing the dry precipitate. This estimate neglects the scattering and moderation effect of the oxygen associated with the dry precipitate, but it indicates that the safe diameter is larger than the extrapolated 8.1 inches. However, water can be added to the cake without appreciably changing the concentration of plutonium thus decreasing the critical diameter to some minimum which is the actual diameter of interest. In other words, there is a certain H/Pu-239 atomic ratio which, for the precipitate-water slurry, is the most reactive and thus takes the smallest critical volume of all the possible concentrations of the precipitate water homogeneous slurries which can be made critical. This particular H/Pu ratio gives the condition called the optimum moderation for plutonium precipitate water slurries.

In order to investigate the condition of optimum moderation some information was received from B. F. Judson on an experiment which was done to study the chemistry of various precipitate cases. They formed a plutonium polymer of $PuO_2(H_2O)_{7-1/2}$ and analyzed their solution for two concentrations of plutonium to get the following results

1. At a plutonium concentration of 400 g/l (H/Pu ~ 52)

   681 g/l of the polymer

   - 61 g/l of $PuO_2(NO_3)_2$
   - 16 g/l of HNO_3
   - 640 g/l of H_2O

2. At a plutonium concentration of 1000 g/l (H/Pu ~ 22)

   1700 g/l of polymer

   solution
   - 26 g/l of $PuO_2(NO_3)_2$
   - 7 g/l of HNO_3
   - 267 g/l of H_2O

   slurry

On further drying this material to (H/Pu ~ 15) they found the concentration did not change but remained about 1000 g/l of plutonium.

By some previous experiments they found that the specific gravity of the $PuO_2(NO_3)_2$ solution could be represented by a formula of the form

$$SP.\ G. = 1 + 0.031\ x + 0.35\ y$$

where x is the molarity of HNO_3 and y is the molarity of the plutonium.

Using this equation and the chemical analysis it is possible to calculate the density (d_p) of the plutonium polymer by the following equation:

$$d_p = \frac{W_p}{1 + 0.031\,x + 0.35\,y - (d_T - W_p)1/d_{H_2O}}$$

where

d_{H_2O} is the density of water

W_p is the polymer weight per cc of slurry

d_T is the total density in grams per cc of the slurry

x and y are defined above

For the data at 400 g/l plutonium this gives d_p = 2.41 g/cc and the 1000 g/l data gives d_p = 2.43 g/cc. This density is the polymer density which can be used to estimate H/Pu ratios for water polymer mixtures whose plutonium concentration is less than one gram per cc. Using the formula of the polymer as $PuO_2(H_2O)_{7-1/2}$, the (H/Pu) atomic ratio for the polymer water mixture is

$$(1) \qquad (H/Pu)_p = \frac{26.53}{C^p_{Pu}} - 3.63 \; ; \; C^p_{Pu} < 1.0 \text{ g/cc}$$

where C^p_{Pu} is the concentration of the plutonium in this mixture.

The case that Safonov used for his calculation of a metal water mixture has an $(H/Pu)_m$ atomic ratio of

$$(2) \qquad (H/Pu)_m = \frac{26.53}{C^m_{Pu}} - 1.679$$

where C^m_{Pu} is the concentration of plutonium in the water metal mixture.

For the water polymer mixture there is no experimental information on the variation of the (H/Pu) ratio at C^p_{Pu} greater than one g/cc so the assumption is made that the variation follows an equation of the form $(H/Pu)_p = \frac{A}{C^p_{Pu}} + B$

with the boundary conditions of

$(H/Pu)_p = 0$ when $C^p_{Pu} = 3.5$ g/cc

$(H/Pu)_p = 22.9$ when $C^p_{Pu} = 1.0$ g/cc

This gives

$$(3) \qquad (H/Pu)_p = \frac{32.06}{C^p_{Pu}} - 9.16 \; ; \; 1 < C^p_{Pu} < 3.5$$

With these three equations it is possible to get the ratio of C^m_{Pu}/C^p_{Pu} at the same H/Pu ratio for various concentrations of the plutonium by setting $(H/Pu)_p = (H/Pu)_m$ to get

$$(4) \qquad \frac{C^m_{Pu}}{C^p_{Pu}} = 0.07354 \; C^m_{Pu} + 1 \; ; \; C^p_{Pu} < 1.0$$

$$(5) \qquad \frac{C^m_{Pu}}{C^p_{Pu}} = 0.2334 \; C^m_{Pu} + 0.8274 \; ; \; 1 < C^p_{Pu} < 3.5$$

The curves published by Safanov can be used to find the bare sphere critical radius (R^m_s) of a metal water mixture with a given $(H/Pu)_m$ and C^m_{Pu}. By equating geometric bucklings of an infinitely long bare cylinder and a bare sphere, the radius of the critical cylinder (R^m_c) containing this material can be estimated by the equation:

$$(6) \qquad R^m_c = (R^m_s + \ell) \frac{2.4048}{\pi} - \ell$$

where ℓ is the bare reactor extrapolation length. Then using the Equations 4 and 5 the estimated critical radius (R^p_c) for an infinite cylinder containing a mixture of water and plutonium polymer is given by

$$R^p_c = R^m_c \left(\frac{C^m_{Pu}}{C^p_{Pu}} \right)$$

The results of this calculation can be sketched as shown in Figure 9.

Figure 9

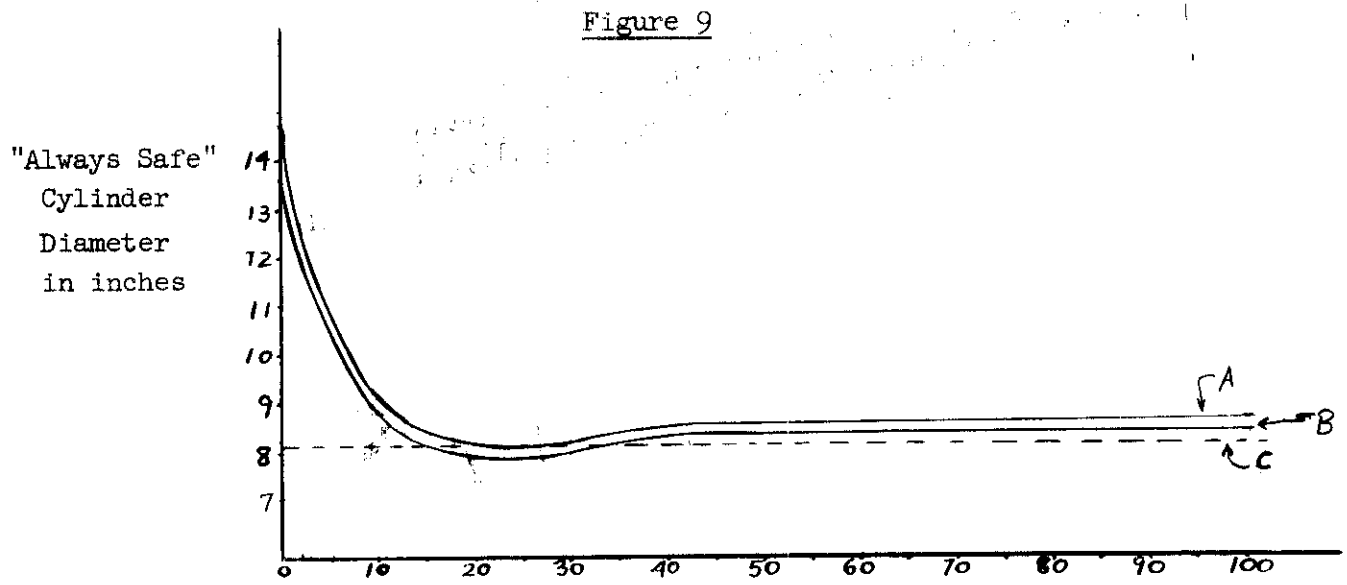

The value of the extrapolation length (ℓ) to use in Equation 6 is uncertain for this problem. Previous estimates on ℓ gave values around 2.68 cm which is the value used to calculate Curve A. However, some calculations done at Los Alamos[22] indicate that the Oak Ridge data are best fit by a bare extrapolation length of 4 cm which is the value used for Curve B in Figure 9. Line C of Figure 9 is the presently used extrapolated value for the "always safe" cylinder diameter. This calculation is also uncertain, as previously noted, since it neglects the moderation and scattering effects of the oxygen which is associated with the precipitate.

Contact has been made with people at Oak Ridge by G. M. Muller and G. W. Anthony to make a calculation similar to that of G. Safanov and to extend these calculations to the precipitate case.

However, there will probably always be some uncertainty in such calculations, since cross sections are adjusted to make the calculation fit experimental data. The best solution to this problem would be an experiment. In Figure 9 it is shown that the mixture of optimum moderation for the precipitate case comes at the H/Pu ratio of ~ 25. The chemists' experiment shows that this is the region in which the Pu density is not changing rapidly as water is added to the mixture. Thus, it is conceivable that the mixture which gives the optimum moderation is the one naturally occurring when the precipitate settles to the bottom of a tank. This indicates the problem is a real one and also suggests an experimental procedure for measuring the minimum critical volume. The experiment could start with the dry polymer (H/Pu ~ 15) and multiplication measurements made as small increments of water are added to the mixture. The volume of this mixture stays essentially constant as the optimum concentration is approached. This avoids the more hazardous experiment in which the mixture is kept homogeneous by a mechanical stirrer such that when the stirrer is shut off the precipitate can settle to an unknown and possibly more reactive configuration. This experiment could be made in a 10" aluminum-walled cylinder so that the height for the bare

(22) W-2-353, Extract

cylinder will nearly equal the diameter. Flux traverses could be made on the critical assembly by using a wire of some activating material such as gold placed in a small re-entrant tube through the center of the cylinder. Scanning this wire with a counter would give the flux distribution and fitting this distribution to the appropriate diffusion theory function would give information on the extrapolation length. This extrapolation length would then be used to interpret the results of the minimum critical volume experiments in terms of a safe column diameter.

In order to do such an experiment, it would be practically necessary to start a critical mass experimental program. It is felt, however, that there are enough problems accumulated which concern the handling of plutonium in the present separation plants to warrant such an experimental program. Some of these problems can be listed as follows:

1. The "always safe" cylinder diameter.

2. The "always safe" slab size.

3. The interaction between safe vessels as a function of distance and reflection between them.

4. The interaction between larger vessels which can be made critical as a function of distance and reflection between them.

5. The effect of joining process pipes onto safe vessels.

6. The effect of adding reflectors in the form of supports to safe cylinders.

7. The effect of Pu-240 on the safe vessel size.

8. The effect of nearby structural materials on the safe vessel size as a function of distance from the vessel.

Items 1 and 2 are related in theory by equating bucklings. However, this calculation is uncertain because of the uncertainty of the extrapolation length as already noted. Possibly such experiments would give another method of finding the extrapolation length for plutonium solutions. Item 3, on the interaction between safe vessels, is a very immediate problem concerning the handling of sample cans and the new PR (product receiving) cans. Present limits on the handling of these cans are very uncertain and hence are made ultraconservative. An experiment would probably allow a considerable increase in these handling limits and storage costs. Item 4, concerning interaction between critical vessels, has been studied at Oak Ridge for $U^{235}O_2F_2$ solutions and the data have been used for problems concerning plutonium solutions. However, because of the plutonium resonance near 0.3 ev, the effect of neutron interaction might be appreciably different for vessels containing plutonium. Similar arguments can also be given for the effect of reflection from supporting pipes. Concerning Item 7, G. Safanov shows in R-259 that the "median fission energy" for an H/Pu ratio of 20 is about 10 ev. This is an energy considerably above the resonance energy of Pu-240 which is about 1 ev. Thus, the effect of Pu-240 could be different for

this case than that which was measured in the previous critical mass experiments.

At present there is an experimental program at Oak Ridge studying the critical mass of various U-235 solutions. However, because of the biological hazards associated with plutonium solutions, they are not equipped to handle plutonium critical mass problems. There have been an increasing number of these problems arising for which only conservative solutions can at present be estimated. It appears that an experimental program would give information on the critical concentration above any previous experiments to study the criticality hazards of continuous flow separations plants, and, also such a program would reduce some of the uncertainties in the present critical mass information, which are causing severe limitations in the handling and storage of plutonium solutions.

W. J. Ozeroff

Manager - Physics Research
ENGINEERING DEPARTMENT

WJ Ozeroff:as